Kovove Mater. 62 2024 245–252
DOI: 10.31577/km.2024.4.245

Kinetics simulation of TiB_2 layers on the titanium alloy (Ti6Al4V) obtained by liquid boriding process

Mohammed Amine Khater[1], Bendaoud Mebarek[2], Sabik Abdelhadi Bouaziz[1], Mourad Keddam[3], Yassine el Guerri[4]

[1]*Laboratoire de Recherche en Technologie de Fabrication Mécanique, École Nationale Polytechnique d'Oran M.A, BP 1523 Oran El M'Naouer, Algeria*
[2]*Laboratoire de Recherche en Intelligence Artificielle et Systems, University of Tiaret, Algeria*
[3]*Laboratoire de Technologie des Matériaux, Faculté de Génie Mécanique et Génie des Procédés, USTHB, B.P. No. 32, 16111, El-Alia, Bab-Ezzouar, Algiers, Algeria*
[4]*Research laboratory of industrial technologies, University of Tiaret, Algeria*

Received 21 February 2022, received in revised form 30 June 2023, accepted 12 September 2024

Abstract

In this study, we conducted a kinetics simulation of TiB_2 layers obtained by the boriding process in the temperature range of 1123–1323 K. To investigate the influence of different boriding parameters, we developed a mathematical model based on Fick's law and the mass balance equation. This model allows us to estimate the boron concentration in the TiB_2 phase, the boride layer thickness, and the mass gain. To validate the simulation results, we compared them with our experimental data on liquid boriding with a salt bath consisting of 70 % Borax (Na2B4O7) and 30 % Silicon carbide (SiC) applied to the titanium alloy (Ti6Al4V). The comparison confirmed the validity of our model, assuring the accuracy of our simulation results.

K e y w o r d s: liquid boriding, titanium borides, kinetics, diffusion model, simulation

1. Introduction

Titanium and its alloys are generally utilized in aviation, petrochemical, car, and biomedical applications owing to their properties, for example, their high strength-to-weight ratio (even at high temperatures), their outstanding biocompatibility, and their great resistance against corrosion and oxidation [1, 2]. In any case, low wear resistance associated with a low hardness limits its utilization, especially in tribological applications, because of the inherent nature of titanium [3, 4]. In this way, a few surface modification methods, for example, nitriding [5], oxidizing [6], and carburizing [7] on titanium surfaces, are considered the adequate methods to improve surface hardness and strength wear of titanium and its alloys.

The boriding technique is frequently utilized for titanium and its alloys to obtain a hard boride layer by thermodiffusion of boron atoms into the metallic substrate [8]. This hard boride layer is produced in the temperature range of 973–1373 K by different techniques, including laser boriding [9], plasma-assisted boriding [10], pack boriding [11], boriding in molten salts [12].

The modeling of boriding kinetics by different approaches is of great importance in controlling the boriding parameters such as the treatment time, the temperature, and the boron concentration [13]. For instance, Campos et al. [14] have used a mathematical model based on Fick's law to estimate the boron diffusion coefficients in the Fe_2B layer formed on Armco iron substrate by the powder-pack boriding. In another model, Keddam et al. [15] proposed a kinetic model based on the integral method to estimate the boron diffusion coefficients in the Fe_2B layers on AISI P20 steel. Kulka et al. [16] have simulated the growth kinetics of FeB and Fe_2B layers on Armco iron substrate produced by the gas boriding in the H_2-BCl_3 atmosphere.

Mebarek et al. [17] have investigated the kinetics of

*Corresponding author: e-mail address: email: mebarekbendaoud@yahoo.fr

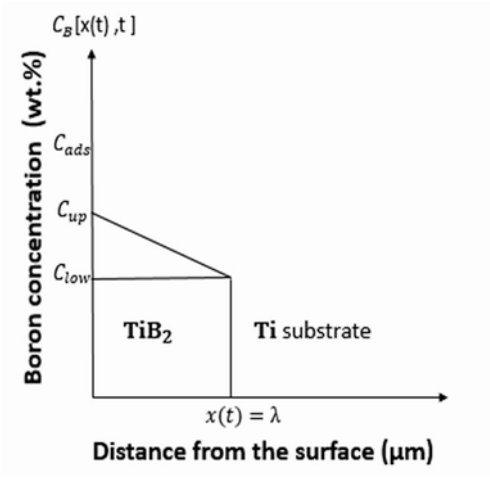

Fig. 1. Schematic representation of the boron concentration profile along the TiB_2 layer.

the formation of Fe_2B layers on AISI 316 steel formed by liquid boriding in a salt bath composed of (70 wt.% Borax and 30 wt.% Silicon carbide) between 1073 K and 1373 K. In their model, the value of activation energy for boron diffusion was estimated as equal to 174.6 kJ mol^{-1} for AISI 316 stainless steel. In another study, Mebareket et al. [18, 19] employed the artificial intelligence technique for simulating the boriding kinetics.

The modeling of the growth kinetics of titanium borides was already detailed by Keddam et al. [20]; the developed model is based on the mass balance equation. This model is used to simulate the layers' thicknesses of TiB_2 and TiB, in which the titanium boride layers were produced by plasma paste boriding on Ti6Al4V at 973–1073 K.

In this paper, the boriding kinetics of Ti6Al4V alloy was investigated. The experimental data obtained by liquid boriding on Ti6Al4V alloy were used [21]. A single-phase layer (TiB_2) at the surface of Ti6Al4V alloy was formed during this process in the temperature range 1123–1273 K.

A mathematical model was suggested to predict the TiB_2 layer thickness, the parabolic growth constant, the boron concentration profile inside the TiB_2 phase, and the mass gain as a function of boriding parameters (see Fig. 1).

2. Simulation model

To simulate the diffusion of boron into the Ti6Al4V alloy, we used the second Fick's law given by Eq. (1):

$$\frac{\partial C_i(x,t)}{\partial t} = D_i \frac{\partial^2 C_i(x,t)}{\partial x^2} \tag{1}$$

with

$$D_i = D_i^0 \exp\left(-\frac{Q}{RT}\right), \tag{2}$$

where D_i^0 is a pre-exponential factor, Q_i represents the activation energy per mole, R is the universal gas constant ($R = 8.314\,\mathrm{J\,mol^{-1}\,K^{-1}}$), and T is the temperature.

The general solution of Eq. (1) for each phase i is given by:

$$C_i(x,t) = A_i + B_i \mathrm{erf}\left(\frac{x}{2\sqrt{D_i t}}\right). \tag{3}$$

The solution of Eq. (3) simulates the boron concentration in the TiB_2 phase, with C_{up} and C_{low} as the upper and lower limits of boron concentrations in the TiB_2 phase. The term C_{ads} represents the adsorbed concentration of boron.

This study considers that the boron concentration is linear through the TiB_2 layer.

To calculate the boron concentration inside the TiB_2 phase, we consider the following conditions:

for $t = t$ and $x = 0$, $C(t,0) = C_{\mathrm{up}}$, if $t > 0$ and $x = \lambda$, $C(t,x) = C_{\mathrm{low}}$.

From this condition, we estimate the boron concentration profile in the TiB_2 phase, where λ is the boride layer thickness of TiB_2.

We use the mass balance equation to calculate the TiB_2 layer thickness based on the expression of mass conservation at the TiB_2/substrate interface. The displacement of the interface is described by Eq. (4):

$$a\frac{\mathrm{d}x}{\mathrm{d}t}\,|_{x=\lambda} = -D_{\mathrm{TiB_2}} \left.\frac{\partial C_{\mathrm{B}}^{\mathrm{TiB_2}}(x,t)}{\partial x}\right|_{x=\lambda} \tag{4}$$

with

$$a = \left[\frac{(C_{\mathrm{up}} - C_{\mathrm{low}})}{2} + (C_{\mathrm{low}} - C_0)\right],$$

where C_0 ($C_0 = 0$) is the boron concentration in the matrix, D is the boron diffusion coefficient in the TiB_2 phase, C_{up} is the upper limit of boron in the TiB_2 phase, while C_{low} denotes the lower value of boron in the TiB_2 layer.

In this study, we consider that the time dependence of TiB_2 layer thickness is expressed by a parabolic law given by Eq. (5):

$$\lambda = k\sqrt{t}, \tag{5}$$

where k represents the growth rate constant.

Table 1. Chemical composition of Ti6Al4V alloy (in mass %)

Al	V	Fe	C	H	N	O	Ti
6.13	3.98	0.15	0.04	0.001	0.011	0.14	Bal

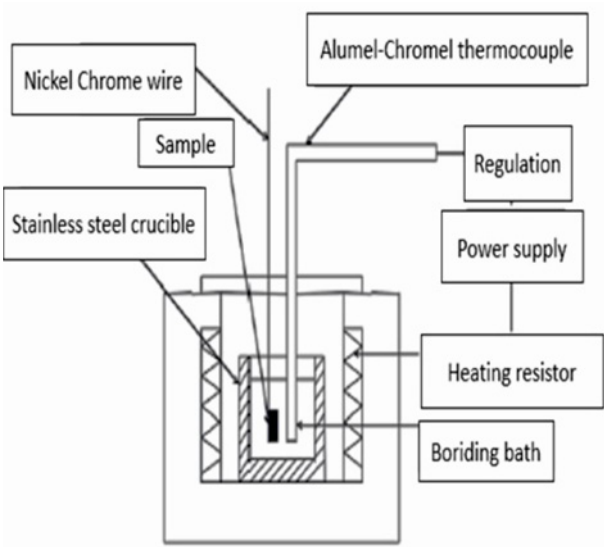

Fig. 2. Boriding device [21].

With the use of previous equations and after the rearrangement of Eq. (4), the expression of boron diffusion coefficients in the TiB_2 layer can be derived as follows:

$$D_{TiB_2} = \frac{k^2}{4}\left(\frac{C_{up} + C_{low}}{C_{up} - C_{low}}\right). \quad (6)$$

The values of upper and lower boron contents in TiB_2 are taken from reference [20], with $C_{up} = 31.10$ wt.% and $C_{low} = 30.10$ wt.%.

3. Experimental procedure

In this experimental study, the Ti6Al4V alloy has been used as a substrate for boriding in a liquid medium [21]. Table 1 shows the chemical composition of this material.

The samples to be borided had a cylindrical shape with a diameter of 10 mm and a length of 12 mm. To avoid any oxidation which can disturb the kinetics of boriding, the surfaces to be borided were polished with silicon carbide paper progressively up to a particle size of 1200 grains cm^{-2} just before boriding treatment. Then, they were washed with distilled water, degreased with ultrasound in acetone, and rinsed with alcohol.

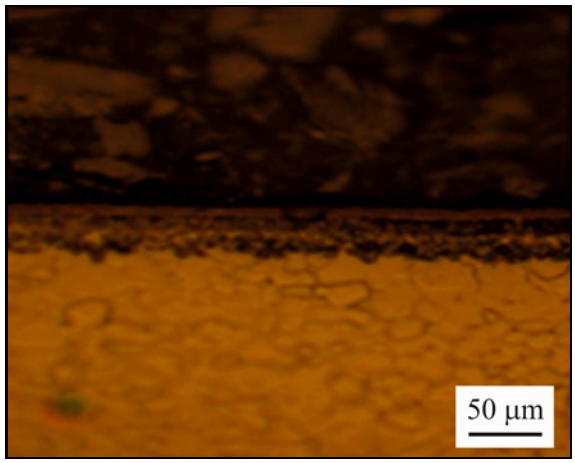

Fig. 3. Optical micrograph of a cross-section of the boride layer obtained at the surface of Ti6Al4V alloy at 1273 K for 8 h.

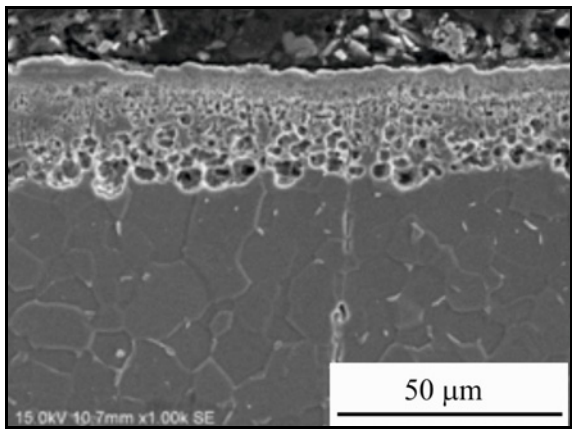

Fig. 4. Observation by scanning electron microscopy of the boride layer at 1273 K for 8 h.

The samples were borided in the open air in a liquid environment by immersion in an electric salt bath oven (Fig. 2). Liquid boriding was carried out in molten salts containing 70 % by weight of $Na_2B_4O_7$ and 30 % by weight of SiC. Three boriding temperatures, 1123, 1223, and 1273 K, were used with 2, 4, 6, and 8 h treatment times. After the boriding treatment, all samples were removed from the furnace, air-cooled to ambient temperature, and cleaned from any residue adhering to the surface (see Figs. 3, 4).

4. Results and discussion

4.1. Evaluation of the activation energy for boron diffusion

To assess the values of boron diffusion coefficients in the TiB_2 layers, the values of parabolic growth con-

Table 2. Calculated values of boron diffusion coefficients in TiB_2 with the corresponding experimental parabolic growth constants

Temperature (K)	Experimental parabolic growth constants ($\mu m\, s^{-0.5}$) [21]	D_{TiB_2} ($m^2\, s^{-1}$) with Eq. (6)
1123	0.0918	1.29×10^{-13}
1223	0.2283	7.97×10^{-13}
1273	0.2825	12.2×10^{-13}

Table 3. Comparison of boron activation energies for titanium alloys by different methods

Materials	Boriding method	Activation energy (kJ mol^{-1})	Ref.
Cp-Ti	Molten-salt	225.617 (TiB_2)	[22]
Cp-Ti	CRTD-boriding	189.9(TiB_2)	[23]
TB2 alloy	Pack boriding	158.056	[24]
Ti6Al4V	Ti6Al4V/Sigma fiber composites	187 (TiB_2) 190 (TiB)	[27]
Ti6Al4V	Pack boriding	231.177 ((TiB_2)	[26]
Ti6Al4V	Plasma paste	136 (TiB_2) 63 (TiB)	[20]
Ti6Al4V	Superplastic boronizing	226.17 (TiB_2)	[25]
Ti6Al4V	Liquid boriding	183.14 (TiB_2)	Present study

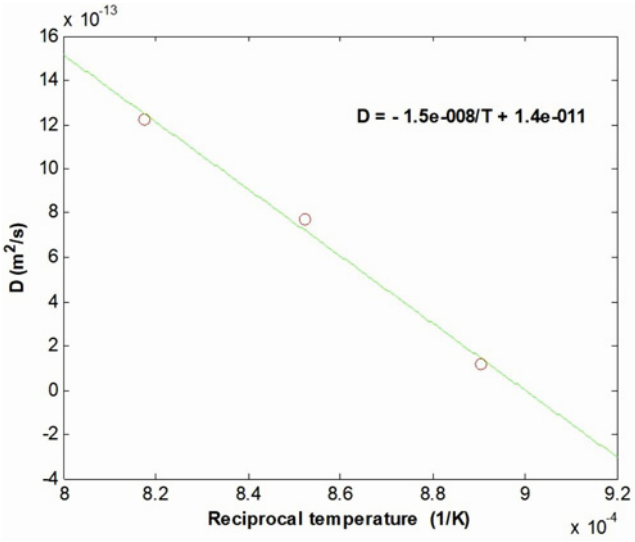

Fig. 5. Temperature dependence of calculated boron diffusion coefficients in TiB_2.

stants derived from the plot of layer thickness against the square root of time are needed.

The experimental parabolic growth constants were obtained based on the kinetic results of Fig. 5 of reference [21]. The estimated values of boron diffusivities for the TiB_2 layer with Eq. (6) are listed in Table 2 for an upper boron content of 31.10 wt.% in TiB_2.

To get the value of boron activation energy in TiB_2, the values of boron diffusion coefficients in the TiB_2 layers were fitted with the Arrhenius equation, as shown in Fig. 5.

From Fig. 5, the value of activation energy for boron diffusion in Ti6Al4V alloy was estimated as 183.14 kJ mol^{-1}. The diffusion coefficient of boron in TiB_2 was fitted with the Arrhenius equation in the temperature range 1123–1273 K. The temperature dependence of the boron diffusion coefficient in TiB_2 in the temperature range 1123–1273 K was given by Eq. (7):

$$D_{TiB_2} = 4.48 \times 10^{-5} \exp\left(-\frac{183.14\ \text{kJ mol}^{-1}}{RT}\right). \quad (7)$$

Table 3 lists the values of the boron activation energies for titanium alloys by different methods and for different materials. From Table 3, the values of the activation energies obtained are dependent on the boriding method (liquid, solid, and gas medium).

Generally, the activation energies depend on the chemical composition of the treated material, the boriding method, and the temperature treatment.

It is seen that the obtained value of boron activation energy in Ti6Al4V alloy is consistent with the results displayed in Table 3.

From Table 3, we can observe different values of the activation energy. Variations in the boriding method and diffusion model employed in different studies can lead to observed differences in activation energies. Different boriding methods can result in variations in the microstructure and composition of the boride layer. The specific conditions, such as the temperature, the time, the boron source, and the atmosphere composition, can influence the diffusion kinetics and the resulting layer characteristics. Generally, to calculate the activation energy, we use many diffusion models to make assumptions about factors like concentration

Table 4. Calculated and experimental growth rate constants k

Growth rate constants ($\mu m\, s^{-1/2}$)		
Temperature (K)	Calculated k ($\mu m\, s^{-1/2}$)	Experimental k ($\mu m\, s^{-1/2}$) [21]
1123	0.0940	0.0918
1223	0.2099	0.2283
1273	0.2990	0.2825

Table 5. Time dependence of the TiB_2 boride layer thickness for increasing temperatures (the results in bold are the simulated values)

Temperature (K) Time (h)	1123	1223	1273
2	7.71/**7.97**	15.21/**17.81**	19.71/**25.37**
4	10.01/**11.28**	26.57/**25.18**	30.85/**35.88**
6	13.07/**13.81**	34.9/**30.84**	42.0/**43.94**
8	16.7/**15.95**	40.8/**35.62**	51.85/**50.74**

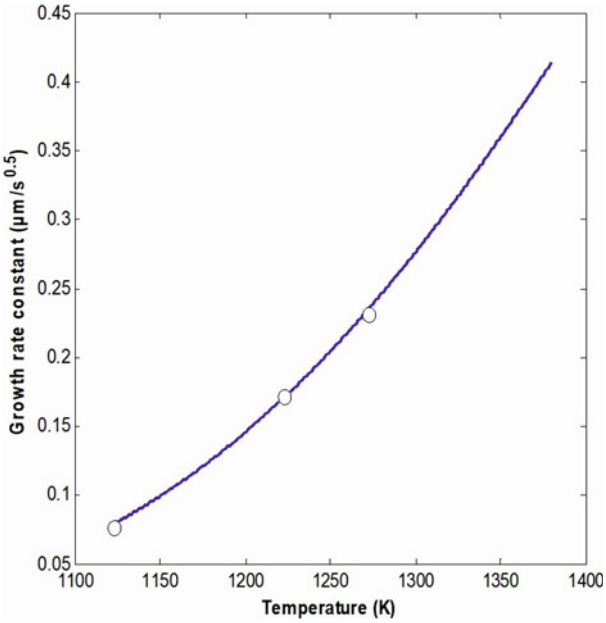

Fig. 6. Evolution of the growth rate constant vs. temperature.

gradients, diffusion paths, and diffusivity. These factors can directly impact the calculated activation energy. Fan et al. [27] studied the reaction kinetics between the TiB, coating, and Ti matrix for the diffusion coefficient calculation. The diffusion mechanisms for B atoms in TiB and TiB_2 have been identified in this study vacancy diffusion; the authors note that the activation energy for boron diffusion in TiB is notably lower along the (0 1 0) TiB direction, which can be regarded as a nearly one-dimensional pathway. Conversely, in TiB_2, the diffusion path predominantly follows the (1 0 0) TiB_2 directions, forming a two-dimensional network.

Therefore, if different studies employ different boriding methods or diffusion models, variations in the observed activation energies would likely arise.

4.2. Kinetic studies

Using the model of the growth kinetics of boride layers mentioned previously, we have implemented a simulation code to calculate the TiB_2 layer thickness and predict the boron concentration profile inside the TiB_2 phase.

The diffusion and thermodynamic data used in this model are the diffusivity of boron in TiB_2 calculated with Eq. (7); the upper limit of boron content in TiB_2 represents the boron concentration at the surface with the value of 31.10 wt.%, the lower limit of boron content in TiB_2 (= 30.10 wt.%).

The comparison between the growth rate constants obtained by simulation and experimental data is shown in Table 4.

We notice a good agreement between our experimental data and the calculated data at 1123, 1223, and 1273 K (the boron concentration at the surface is C_{up} = 31.10 wt.% B).

There is a good agreement between the simulated growth rate constants and experimental values of parabolic growth constants. The growth kinetics of the boride layer increases with the temperature.

Table 5 compares the experimental values of TiB_2 layer thickness and the simulated thicknesses for an upper boron content of 31.10 wt.% in TiB_2. It is seen that the experimental data [21] are in line with the simulated results.

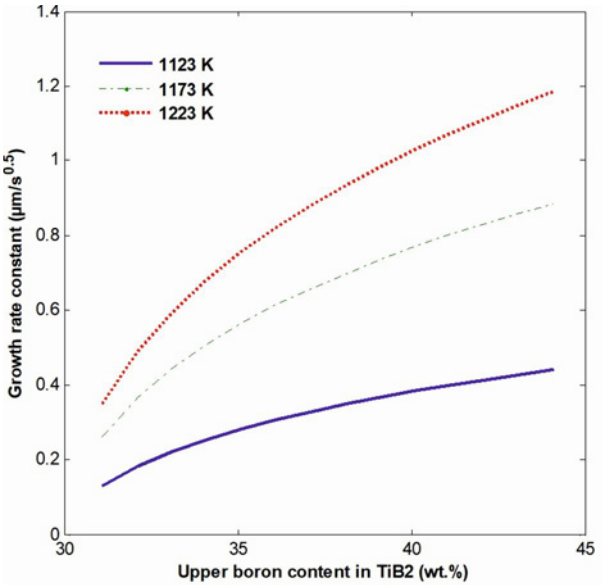

Fig. 7. Variation of simulated growth rate constant as a function of upper boron content in TiB_2.

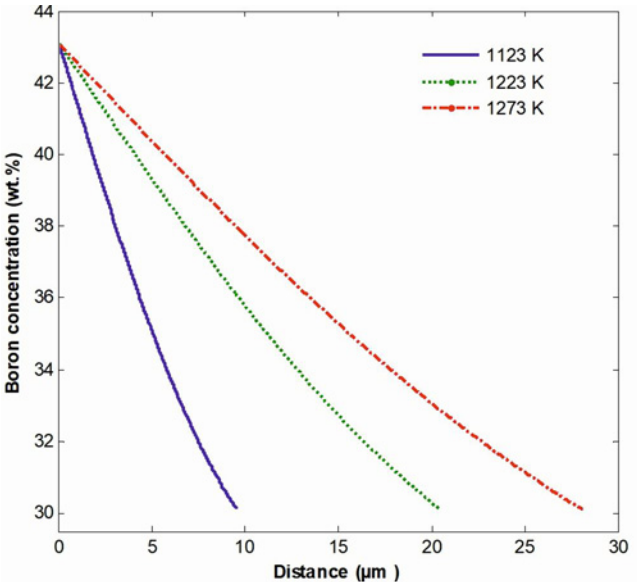

Fig. 8. Calculated boron concentration profiles along the TiB_2 layer for a treatment time of 4 h at increasing temperatures with an upper boron content of 43.10 wt.% in TiB_2.

The simulated values of TiB_2 layer thickness indicated in bold in Table 5 are between 8.76 and 57.9 μm. It is also noted that the TiB_2 layer thickness increases with the temperature rise for a given treatment time.

Generally, the boriding of the titanium leads to the formation of TiB_2 and TiB instantly; the TiB layer is very thin compared to the TiB_2 in the case of bilayer configuration, we will obtain the bilayer configuration with an important layer thickness of TiB if we increase the boron concentration in the surface.

In practice, it is difficult to experimentally measure the boride layer thickness from the optical microscope investigation; this difficulty arises from the microstructural nature of the interface (boride layer/substrate).

Figure 7 describes the variation of the simulated growth rate constant as a function of the upper boron concentration in TiB_2 at the material surface. This figure evaluates the parabolic growth rate constant for the concentration between C_{low} and the boron concentration of 43.10 wt.%.

From Fig. 7, we note that the growth rate constant increases with the rise of upper boron concentration in TiB_2. This leads to an increase in the boride layer thickness.

The boron concentration at the surface plays an important role in the kinetics of the boriding process.

The surface boron concentration is a key parameter responsible for accelerating or optimizing the boriding process and has to be chosen based on different criteria (the boride layer's thickness and the duration of the process). With increasing temperature, the diffusion process proceeds quickly through the borided layer.

In Fig. 8, the calculated boron concentration profiles along the TiB_2 layer are plotted for 4 h at increasing temperatures using Eq. (3). The boron content in the TiB_2 phase changes with the boriding temperature. At high temperatures, the boron content rapidly attains a limit value of the boron concentration in the TiB_2 phase required for its development and growth.

The mass gain per unit area is evaluated using Eq. (8). The calculation is based on the assumption that the TiB_2 layer is formed instantly at $t = 0$ and immediately covers the surface:

$$G(t) = 2\rho \frac{(C_{\text{up}} - C_{\text{low}})}{\operatorname{erf}\left(k/2\sqrt{D_{\text{TiB}_2}}\right)} \sqrt{\frac{D_{\text{TiB}_2}}{\pi}} t, \qquad (8)$$

where $G(t)$ represents the mass gain (g cm^{-2}) and ρ is the titanium density ($= 4.506\,\text{g cm}^{-3}$).

Figure 9 shows the time dependence of mass gain associated with forming the TiB_2 layer at the surface of the Ti6Al4V alloy for increasing temperatures with an upper boron content of 31.10 wt.% in TiB_2. Figure 9 shows that the mass gain increases with the boriding temperature.

5. Conclusions

In this study, a mathematical diffusion model is applied to simulate the growth kinetics of the TiB_2 layer formed on Ti6Al4V alloy by liquid boriding in the temperature range 1123–1273 K. By analyzing the kinetics data, the value of activation energy for boron diffusion

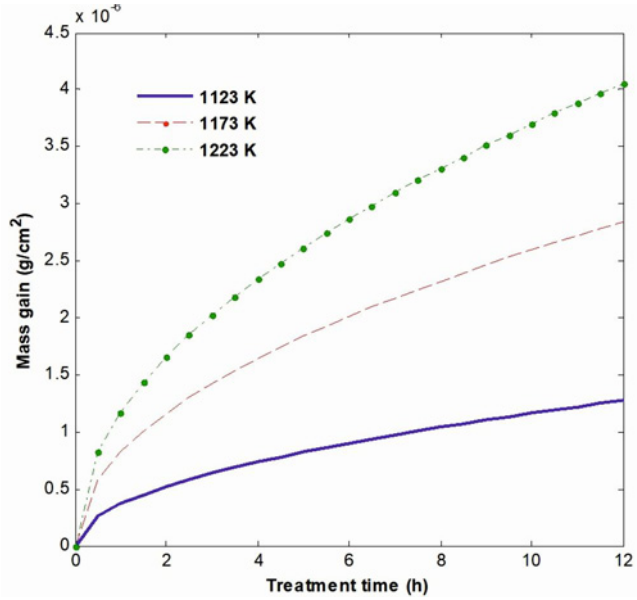

Fig. 9. Time dependence of mass gain recorded at the surface of Ti6Al4V alloy for increasing temperatures.

in Ti6Al4V alloys was estimated as 183.14 kJ mol^{-1}. This value of energy was compared to the literature data.

Our simulation model can predict the boron concentration profile inside the TiB_2 phase and its layer thickness. With this simulation, we can estimate the influence of different parameters such as the temperature, the boriding duration, and the upper boron concentration in TiB_2 at the material surface on the boriding kinetics of Ti6Al4V alloy. Finally, the simulation results were in good agreement with the experimental data.

References

[1] L. M. Agrini, H. J. Rack, Titanium alloys in total joint replacement – a materials science perspective, Biomaterials 19 (1998) 1621–1639. https://doi.org/10.1016/S0142-9612(97)00146-4

[2] C. Leyens, M. Peters, Titanium and Titanium Alloys, Fundamentals and Applications, John Wiley & Sons, 2003. ISBN:9783527305346

[3] C. Fei, Z. Hai, C. Chen, X. Yangjian, Study on the tribological performance of ceramic coatings on titanium alloy surfaces obtained through micro-arc oxidation, Prog. Org. Coat. 64 (2008) 264–267. https://doi.org/10.1016/j.porgcoat.2008.08.034

[4] C. Lee, A. Sanders, N. Tikekar, K. S. R. Chandran, Tribology of titanium boride-coated titanium balls against alumina ceramic: Wear, friction, and micromechanisms, Wear 265 (2008) 375–386. https://doi.org/10.1016/j.wear.2007.11.011

[5] W. Chou, G. Yu, J. Huang, Mechanical properties of TiN thin film coatings on 304 stainless steel substrates, Surf. Coat. Technol. 149 (2002) 7–13. https://doi.org/10.1016/S0257-8972(01)01382-2.

[6] L. S. Dubrovinsky, N. A. Dubrovinskaia, V. Swamy, J. Muscat, N. M. Harrison, R. Ahuja, B. Holm, B. Johansson, The hardest known oxide, Nature 410 (2001) 653–654. https://doi.org/10.1038/35070650

[7] L. R. Katipelli, A. Agarwal, N. B. Dahotre, Laser surface engineered TiC coating on 6061 Al alloy: microstructure and wear, Appl. Surf. Sci. 153 (2000) 65–78. https://doi.org/10.1016/S0169-4332(99)00368-2

[8] M. Elias-Espinosa, M.Ortiz-Domínguez, M. Keddam, O. A. Gómez-Vargas, A. Arenas-Flores, Boriding kinetics and mechanical behaviour of AISI O1 steel, Surf. Eng. 31 (2011) 588–597. https://doi.org/10.1179/1743294415Y.0000000065

[9] M. Kulka, M. Makuch, P. Dziarski, D. Mikołajczak, D. Przestacki, Gradient boride layers formed by diffusion carburizing and laser boriding, Opt. Lasers Eng. 67 (2015) 163–175. https://doi.org/10.1016/j.optlaseng.2014.11.015

[10] P. Kaestner, J. Olfe, K. T. Rie, Plasma-assisted boriding of pure titanium and TiAl6V4. Surf. Coat. Technol., Proceedings of the 7th International Conference on Plasma Surface Engineering 2001, pp. 248–252. ISSN 0257-8972. https://doi.org/10.1016/S0257-8972(01)01244-0

[11] M. Bektes, A. Calik, N. Ucar, M. Keddam, Pack-boriding of Fe-Mn binary alloys: Characterization and kinetics of the boride layers, Mater. Charact. 61 (2010) 233–239. https://doi.org/10.1016/j.matchar.2009.12.005

[12] K. Matiašovský, M. Chrenková-Paučírová, P. Fellner, M. Makyta, Electrochemical and thermochemical boriding in molten salts, Surf. Coat. Technol. 35 (1988) 133–149. https://doi.org/10.1016/0257-8972 (88)90064-3.

[13] B. Mebarek, S. A. Bouaziz, A. Zanoun, Simulation model to study the thermochemical boriding of stainless steel "AISI 316" (X5CrNiMo17-12-2), Matér. Tech. 100 (2012) 167–175. (in French) https://doi.org/10.1051/mattech/2012009

[14] I. Campos-Silva, M. Ortiz-Domínguez, H. Cimenoglu, R. Escobar-Galindo, M. Keddam, M. Elías-Espinosa, N. López-Perrusquia, Diffusion model for growth of Fe_2B layer in pure iron, Surf. Eng. 27 (2011) 189–195. https://doi.org/10.1179/026708410X12550773057820

[15] M. Keddam, M. Ortiz-Dominguez, M. Elias-Espinosa, A. Arenas-Flores, J. Zuno-Silva, D. Zamarripa-Zepeda, O. A. Gomez-Vargas, Kinetic investigation and wear properties of Fe_2B layers on AISI 12L14 steel, Metall. Mater. Trans. A 49 (2018) 1895–1907. https://doi.org/10.1007/s11661-018-4535-1

[16] M. Kulka, N. Makuch, A. Pertek, L. Małdziński, Simulation of the growth kinetics of boride layers formed on Fe during gas boriding in H_2-BCl_3 atmosphere, J. Solid State Chem. 199 (2013) 196–203. https://doi.org/10.1016/j.jssc.2012.12.029

[17] B. Mebarek, D. Madouri, A. Zanoun, A. Belaidi, Simulation model of monolayer growth kinetics of Fe_2B phase, Mater. Tech. 103 (2015) 703. https://doi.org/10.1051/mattech/2015058.

[18] B. Mebarek, M. Keddam, A fuzzy neural network approach for modeling the growth kinetics of FeB and Fe_2B layers during the boronizing process, Mater.

Tech. 106 (2018) 603.
https://doi.org/10.1051/mattech/2019002
[19] B. Mebarek, A. Zanoun, A. Rais, Comparison of two numerical approaches for the thermochemical boriding treatment of XC38 steel, Metall. Res. Technol. 113 (2016) 104. https://doi.org/10.1051/metal/2015046
[20] M. Keddam, S.Taktak, Characterization and diffusion model for the titanium boride layers formed on the Ti6Al4V alloy by plasma paste boriding, Appl. Surf. Sci. 399 (2017) 229–236.
https://doi.org/10.1016/j.apsusc.2016.11.227
[21] M. A. Khater, S. A. Bouaziz, M. A. Garrido, P. Poza, Mechanical and tribological behaviour of titanium boride coatings processed by thermochemical treatments, Surf. Eng. 37 (2020) 101–110.
https://doi.org/10.1080/02670844.2020.1763765
[22] L. S. Ma, Y. H. Duan, P. Li, Microstructure, growth kinetics and some mechanical properties of boride layers produced on pure titanium by molten-salt boriding, J. Mater. Eng. Perform. 26 (2017) 4544–4555.
https://doi.org/10.1007/s11665-017-2884-3
[23] G. Kartal, S. Timur, Growth kinetics of titanium borides produced by CRTD-Bor method. Surf. Coat. Technol., Proceedings of the 39th International Conference on Metallurgical Coatings and Thin Films (ICMCTF) 215 (2013) 440–446.
https://doi.org/10.1016/j.surfcoat.2012.08.076.
[24] P. Li, D. Liu, W. Bao, L. Ma, Y. Duan, Surface characterization and diffusion model of pack borided TB_2 titanium alloy, Ceram. Int. 44 (2018) 18429–18437.
https://doi.org/10.1016/j.ceramint.2018.07.060
[25] N. T. Taazim, I. Jauhari, Y. Miyashita, M. F. M. Sabri, Development and kinetics of TiB_2 layers on the surface of titanium alloy by superplastic boronizing, Metall. Mater. Trans. A 47 (2016) 2217–2222.
https://doi.org/10.1007/s11661-016-3359-0
[26] Y. Duan, P. Li, Z. Chen, J. Shi, L. Ma, Surface evolution and growth kinetics of Ti6Al4V alloy in pack boriding, Journal of Alloys and Compounds 742 (2018) 690–701.
https://doi.org/10.1016/j.jallcom.2018.01.383
[27] Z. Fay, Z. X. Guo, B. Cantor, The kinetics and mechanism of interfacial reaction in sigma fibre-reinforced Ti MMCs, Compos. A: Appl. Sci. Manuf. 28 (1997) 131–140.
https://doi.org/10.1016/S1359-835X(96)00105-4